Hydrol. Earth Syst. Sci. Discuss., 7, 9327–9365, 2010
www.hydrol-earth-syst-sci-discuss.net/7/9327/2010/
doi:10.5194/hessd-7-9327-2010

Hydrology and Earth System Sciences Discussions

Channel network identification from high-resolution DTM: a statistical approach

G. Sofia[1], P. Tarolli[1,2], F. Cazorzi[3], and G. Dalla Fontana[1]

[1]Department of Land and Agroforest Environments, University of Padova, Agripolis, viale dell'Università 16, 35020 Legnaro, PD, Italy
[2]Institute of Inland Waters, Hellenic Center for Marine Research, Anavyssos, Greece
[3]Department of Agriculture and Environmental Science, University of Udine, via delle Scienze 208, 33100 Udine, UD, Italy

Received: 17 November 2010 – Accepted: 25 November 2010 – Published: 7 December 2010

Correspondence to: G. Sofia (giulia.sofia@unipd.it)

Published by Copernicus Publications on behalf of the European Geosciences Union.

Abstract

A statistical approach to LiDAR derived topographic attributes for the automatic extraction of channel network is presented in this paper. The basis of this approach is to use statistical descriptors to identify channel where terrain geometry denotes significant convergences. Two case study areas of different morphology and degree of organization are used with their 1 m LiDAR Digital Terrain Models (DTMs). Topographic attribute maps (curvature and openness) for different window sizes are derived from the DTMs in order to detect surface convergences. For the choice of the optimum kernel size, a statistical analysis on values distributions of these maps is carried out. For the network extraction, we propose a three-step method based (a) on the normalization and overlapping of openness and minimum curvature in order to highlight the more likely surface convergences, (b) a weighting of the upslope area according to such normalized maps in order to identify drainage flow paths and flow accumulation consistent with terrain geometry, (c) the *z*-score normalization of the weighted upslope area and the use of *z*-score values as non-subjective threshold for channel network identification. As a final step for optimal definition and representation of the whole network, a noise-filtering and connection procedure is applied. The advantage of the proposed methodology, and the efficiency and accurate localization of extracted features are demonstrated using LiDAR data of two different areas and comparing both extractions with field surveyed networks.

1 Introduction

Recent advances in data collection technology, such as airborne and terrestrial laser scanning, enabled rapid, accurate, and effective acquisition of topographic information (Ackermann, 1999; Kraus and Pfeifer, 2001; Briese, 2004; Slatton et al., 2007; Tarolli et al., 2009). A new generation of high resolution (~1 m) Digital Terrain Models (DTMs) is nowadays widely available, offering new opportunities for the scientific

HESSD

7, 9327–9365, 2010

Channel network identification from high-resolution DTM: a statistical approach

G. Sofia et al.

community to use detailed representations of surfaces. Terrain geometry defines flow paths across a watershed, and raster-based DTMs have been widely applied to derive topographic features by using primary topographic attributes as slope, aspect, and curvature (Florinsky, 1998). The accuracy of feature identification depends on that of the initial dataset, but remains a challenge, partly due to the multi-scale nature of geo-morphological processes and partly due to the absence of objective thresholds for features classification.

Extracting drainage networks from DTMs is one of the most important digital terrain analysis. Traditionally, extraction methodologies are based on the flow routing model. Various drainage algorithms (O'Callaghan and Mark, 1984; Quinn et al., 1991; Tarboton, 1997; Orlandini et al., 2003) offer possibilities of computing drainage networks all over the raster surface. They generally follow the procedure of filling pits, computing flow direction, and computing the contributing area draining to each grid cell (Tarboton, 2003). An alternative to the initial filling procedures is the use of least cost drainage paths (Hart et al., 1968; Ehlschlaeger, 1989). A comparison between traditional sink filling and more recent techniques applied on a radar derived DTM, has been carried out by Metz et al. (2010).

However, the conversion from a drainage flow path to a meaningful network requires a further step. The traditional approach is to use a unique contributing area or slope-area threshold beyond which the hydrographical network is chosen (O'Callaghan and Mark, 1984; Tarboton et al., 1991; Montgomery and Dietrich, 1994; Dietrich et al., 1993; Dalla Fontana and Marchi, 2003). Alternatively, some authors proposed topological or physical reasoning to establish this threshold (Tarboton et al., 1991; Montgomery and Dietrich, 1988). All these approaches share the idea that flow direction is strictly dependent from topographic surface, but one must note that physical location of channel heads, in some situation, is not related just to topographic slope, but depends on several factors as geomorphic processes involved, soil properties, climatic environment, land use etc. (Montgomery and Dietrich, 1988; Prosser, 1996; Wemple et al., 1996; Beven and Kirby, 1979; McGlynn and McDonnel, 2003). In these situations, the

HESSD
7, 9327–9365, 2010

identification of hillslope-to-valley transition between divergent to convergent surfaces according to the slope-area relationship does not necessarily correspond to the actual channel head location (Tarolli and Dalla Fontana, 2009) and a unique value for the area or slope-area thresholds relationship is not enough to characterize all channels (Passalacqua et al., 2010b).

Recently, some authors underlined the effectiveness of specific geometric properties of the topographic surface calculated directly from DTMs to avoid the thresholding issue of classical methods on channel network extraction. Tarboton and Ames (2001) suggested identification of local curvature to account spatially variable drainage density. Upwards curved grid cells have been used by other authors to derive channel networks from digital elevation data (Band, 1986; Gallant and Wilson, 2000). Tarboton (2003) proposed a procedure based on upwards curved grid cells quantification in order to provide a weight matrix to apply on drainage area computation. He suggested the use of a statistic threshold based on the constant drop property of channel networks (Broscoe, 1959) in order to chose the most suitable weighted support area threshold to map channels. According to this procedure, the constant drop property is assumed to be constant along the Strahler order and it is considered as a threshold because it represents the physical transition from channel to hillslope erosion. However, some authors argued that this thresholding procedure is not applicable when the network topology needs to be related to morphology (Thommeret et al., 2010).

The idea of extracting networks only where the terrain express a well defined morphology has been recently proved to allow a more robust geometric positioning of extracted features if compared to the classic approaches. The core idea is to label convergent cells and connect them on a second step using classical flow routing procedures or cost functions based upon them. Wavelet analysis to locally filter LiDAR elevation data and to detect threshold of topographic curvature and slope-direction change has been used by Lashermes et al. (2007) to define valleys and portions of probable channelized areas within the valley. Curvature maps derived from LiDAR DTM have been used by Tarolli and Dalla Fontana (2009) and Pirotti and Tarolli (2010)

HESSD
7, 9327–9365, 2010

to assess the capability of high resolution topography for the recognition of convergent hollow morphology of channel heads and for channel network extraction. Thommeret et al. (2010) used a combination of terrain morphology indices and a single flow drainage algorithm to extract badlands thalwegs network from regular grid DTMs. Passalacqua et al. (2010a,b) applied nonlinear diffusion filtering combined with a geomorphically-informed geodesic cost function to automatically identify channel initiation points and extract channel paths from LiDAR data.

For the present work, we proposed a methodology based on the use of normalized DTM derivatives such as topographic openness (Yokoyama et al., 2002; Prima et al., 2006) and minimum curvature (Evans, 1979) as a weight for the upslope area We propose a three-step method based (a) on the normalization of the two parameters to highlight surface convergences, (b) a weighting of the upslope area according to such normalization to identify the more likely drainage flow paths, and (c) the choice of a statistical parameters as objective threshold for channel head and channel network identification.

2 Study and test sites

We selected two main study sites based on the availability of high-resolution, LiDAR-derived DTMs and detailed independent field based network location datasets. The main study site (Cordon), is a geometrically simple shaped area, defined intuitively in order to include a network and a pour point (maximum flow convergence), without any a-priori reference to a single well defined hydrological unit. The test area instead, refers to a more complex form: an headwater catchment (Miozza). This choice has been done in order to show the accuracy and the objectivity of the proposed methodology for alpine environment with a complex morphology.

The main study area refers to a rectangular selected area (1.4 km^2) located in the Rio Cordon basin (Figs. 1a and 2), an headwater alpine catchment in the Dolomites. Available data of this area consist of several field surveys conducted during the past few

HESSD
7, 9327–9365, 2010

years, including LiDAR survey (data acquired during snow free conditions in October 2006) and DGPS (Differential Global Positioning System) ground observations carried out in 1995–2001 (Dalla Fontana and Marchi, 2003) and during summer 2008–2009 (Pirotti and Tarolli, 2010).

The test area refers to the headwater catchment of Miozza basin (b, Fig. 1): the area covers 4.4 km^2. Basin elevation ranges from 834 to 2075 m a.s.l. with an average value of 1530 m a.s.l. Geomorphological settings of the basin are typical of north-eastern alpine region: deep valleys with high value of slope and significative erosion areas; soil thickness varies between 0.2 m and 0.5 m on topographic spurs to depths of up 1.5 m in topographic hollows. The basin is quite wild and the only significant human activity is related to occasional forest practices. Available data consist of field surveys conducted during the past few years (Tarolli and Tarboton, 2006), including LiDAR survey (data acquired during snow free conditions in 2003) and a DGPS field campaign conducted during 2006–2007 (Tarolli and Dalla Fontana, 2009).

Channel heads were mapped on the field for both areas (Pirotti and Tarolli, 2010; Tarolli and Dalla Fontana, 2009): contributing area at channel head location varies significantly. For the Cordon area, it ranges between approximately 110 m^2 to 13 000 m^2 with an average value of 3099 m^2 and a median value of 1002 m^2 (Passalacqua et al., 2010b). Same analyses carried out for the Miozza basin, show values of contributing area ranging from 128.6 m^2 to 96 680 m^2, with an average value of 6956.95 m^2 and a median value of 1481.67 m^2 (Tarolli and Dalla Fontana, 2009). Considering this high variability, area and slope-area threshold procedures using a unique value have been proved to be not reliable for channel network extraction if compared with the real channel network, especially in areas morphologically complex (Passalacqua et al., 2010b).

3 Topographic attributes

The objective of the work is to delineate the network where surface denotes areas where flows can converge. A large number morphological indexes directly derived

HESSD
7, 9327–9365, 2010

from LiDAR DTMs that enables the identification of terrain convergences exists (Gallant and Wilson, 2000) and some have already been used for network extraction (Tarboton and Ames, 2001; Molloy and Stepinski, 2007; Lashermes et al., 2007; Tarolli and Dalla Fontana, 2009; Pirotti and Tarolli, 2010; Passalacqua et al., 2010a,b). For the present work, flow convergence has been evaluated through a multiple flow direction algorithm (Quinn et al., 1991), while local concavity has been analyzed through two primary topographic attributes: openness (Yokoyama et al., 2002) and minimum curvature according to Evans' (1979) formulation.

3.1 Upslope area

For the present work, we decided to use a multiple flow direction algorithm for upslope area evaluation (Quinn et al., 1991). Several studies have shown differences connected to the choice of single- and multiple-flow direction algorithms on predicting channel networks (McMaster, 2002; Endreny and Wood, 2003), on the location of ephemeral gullies (Desmet and Govers, 1996), on modeled erosion and sedimentation rates (Schoorl et al., 2000), spatial patterns of saturated areas (Guntner et al., 2004), and on the statistical distributions of terrain attributes (Quinn et al., 1991; Wolock and McCabe, 1995; Desmet and Govers, 1996; Tarboton, 1997). Locations of ephemeral gullies and channel networks are better identified by algorithms with limited flow divergence, but upslope area computed through multiple flow algorithms could make it possible the identification parts of channels likely to be active also under conditions of low or moderate flow and it allows the recognition of minor channel features which are involved in flow processes during floods. Multiple direction algorithms (MDF) tend to produce a dispersive flow patterns but at the same time they produce a more realistic looking spatial patterns than the single flow ones by avoiding concentration to distinct lines (Seibert and McGlynn, 2007). The main disadvantage of the base MDF algorithm is that the area from one cell is routed to all downslope cells and thus is dispersed to a large degree even for convergent hillslopes. Flow randomization and concentration can be implemented (Schwanghart and Kuhn, 2010) providing correction to this unrealistic behavior and other algorithms based on triangular facets have been developed to overcome these weaknesses (Tarboton, 1997; Seibert and McGlynn, 2007).

3.2 Minimum curvature

For any two dimensional continuous surface Evans (1972, 1979, 1980) considers five terrain parameters corresponding to groups of 0, 1st and 2nd order differentials, where the 1st and 2nd order functions have components in the xy and orthogonal planes. Curvature is the second spatial derivative of the terrain. Generally the most appropriate curvature form depends on the nature of the surface patch being modelled.

The general concept is to approximate surfaces to a bi-variate quadratic function in the form (Evans, 1979):

$$Z = ax^2 + by^2 + cxy + dx + ey + f \quad (1)$$

where x, y, and Z are local coordinates, and a to f are quadratic coefficients.

Other algorithms for calculating land surface curvature(s) have been referenced (Evans, 1972; Horn, 1981; Zevenbergen and Thorne, 1987; Mitasova and Hofierka, 1993; Shary et al., 2002). However, Evans' (1979) method is one of the most suitable at least for first-order derivatives (Shary et al., 2002) and it performs well in the presence of elevation errors (Albani et al., 2004; Florinsky, 1998).

The two most frequently calculated forms are profile and plan curvature (Gallant and Wilson, 2000). These two measures involve the calculation of the slope vector, therefore they remain undefined for quadratic patches with zero gradient (i.e., the planar components d and e are both zero). In such cases, alternative measures independent from slope need to be substituted. Evans (1979) suggests two measures of minimum and maximum curvature:

$$C_{\max} = -a - b + \sqrt{(a-b)^2 + c^2} \quad (2)$$

$$C_{\min} = -a - b - \sqrt{(a-b)^2 + c^2} \quad (3)$$

The coefficients in Eq. (1) can be solved within a moving window using simple combinations of neighbouring cells: the standard method to solve them involves calculating the parameters for a central cell, related to its eight neighbours in a moving 3×3 cell window.

To perform terrain analysis across a variety of spatial scales different authors (Yokoya and Levine, 1989; Wood, 1996) solved the bi-quadratic equation using a $n \times n$ window with a local coordinate system (x, y, z) defined with the origin at the pixel of interest (central pixel).

Calculation of curvature using a local window is scale dependent, therefore Eqs. (2) and (3) are modified by generalizing the calculation for different window sizes (Wood, 1996):

$$C_{\max} = n \cdot g \left(-a - b + \sqrt{(a-b)^2 + c^2} \right) \tag{4}$$

$$C_{\min} = n \cdot g \left(-a - b - \sqrt{(a-b)^2 + c^2} \right) \tag{5}$$

where g is the grid resolution of the DTM, and n is the size of the moving window.

These two formulae have been widely used in literature for multi-scale terrain analysis (Wilson et al., 2007) and for morphometric feature parameterization (Eshani and Quiel, 2008) since they are directly related to geomorphologic form, where surface concavities and convexities are detected. A mean curvature (C_{mean}) derived from these two formulae has been used by Pirotti and Tarolli (2010) for channel network extraction. Cavalli and Marchi (2008) applied the same generalization procedure to plan curvature formulation, for the characterization of surface morphology.

Channelized landform elements are formed around depressions in curvature and are thus referred to as concave elements, therefore we decided to use $C_{\min}$ (Eq. 5) as optimal for feature recognition (Figs. 7c and 8c). A progressively increasing moving window size (from 3×3 to 33×33 cells) has been considered for the calculation of curvature, in order to reduce the effect of noise and small scale variation in the DTM (Fig. 3a).

3.3 Openness

Openness is a morphometric parameter developed by Yokoyama et al. (2002), expressing the degree of dominance or enclosure of a location on an irregular surface. It is an angular measure of the relation between surface relief and horizontal distance (Prima et al., 2006).

Topographic openness is calculated as the average of either zenith (ϕ) or nadir (ψ) angles along eight azimuths D (0, 45, 90, 135, 180, 225, 270 and 315) within a radial distance L (Yokoyama et al., 2002). Openness always assumes a positive sign and its values range from 0 to 180°. The parameter is designated "*positive*" and "*negative*" in the same sense as it has been used to express terrain-slope curvature (Pike, 1988): positive openness ϕ_L is convex-upward and refers to calculation with zenith angles; negative openness ψ_L is concave-upward and refers to evaluation with nadir angles (Yokoyama et al., 2002).

Along the azimuth D the zenith angle ${}_D\phi_L$ at a grid within radial distance L is

$${}_D\phi_L = 90 - {}_D\beta_L \quad (6)$$

and the nadir angle ${}_D\psi_L$ is

$${}_D\psi_L = 90 - {}_D\delta_L \quad (7)$$

Positive openness ϕ_L of a location on the surface within a distance L on DTMs is

$$\phi_L = ({}_0\phi_L + {}_{45}\phi_L + \ldots {}_{315}\phi_L)/8 \quad (8)$$

and negative openness ψ_L within the L distance is

$$\psi_L = ({}_0\psi_L + {}_{45}\psi_L + \ldots {}_{315}\psi_L)/8 \quad (9)$$

HESSD
7, 9327–9365, 2010

Representation of positive openness are designed to highlight topographic convexities, showing higher openness values for ridges and lower values for concavities, maps of negative openness emphasize drainages (higher values) at the expense of convex-overall features (Yokoyama et al., 2002) (Figs. 7a,b and 8a,b).

To perform terrain analyses maintaining homogeneity with curvature evaluation, openness maps have been carried out considering $n \times n$ moving window (Wood, 2009) (Fig. 3b). Instead of a radial distance L, we considered the distance between the centre of the central pixel and the centre of surrounding ones considered within the window size (n).

4 Kernel size evaluation

A naturally measured sample, according to the central limit theorem (Duda et al., 2001) tends to lead to a normal distribution. Values of the elevation of a smoothed terrain tend to have a symmetric distribution in a well selected window with slow-changing terrain (Bartels et al., 2005). Differently, in the presence of noises and terrain roughness, such a histogram tend to be more or less skewed to one side. Skewness of original elevation data can influence the shape of the distribution of derived topographic attributes: selecting an appropriate window is therefore critical. In a flat region, this window can be fixed and selected a priori, but in a complex and hilly region, imbalanced terrain elevation affects the histogram distribution and increases or decreases the distribution skewness (Yuan et al., 2008).

For this work, the channel pattern recognition and classification is based on the assumption that a deviation of values from their normal distribution can delineate a threshold between well organized valley axes and occurrence of localized convergent topography (Lashermes et al., 2007). This evaluation is carried out through the analysis of a graphical representation of distributions (Chap. 5). To underpin the basis assumptions of the work, meaningful measure are required to describe distributions properly and to describe how kernel size can affect them. The shape of a distribution can be quantitatively described according to its moments: the first moment refers to its mean, the second to its variance (the positive square root of which is the standard deviation, σ), the third and fourth moments refers, respectively to skewness and kurtosis. Tarolli and Dalla Fontana (2009) showed the effectiveness of standard deviation as a threshold value for channel heads identification and the efficiency of statistical values of distribution as threshold for feature extraction on similar areas have been proved by Pirotti and Tarolli (2010).

For our network extraction procedure, skewness (Eq. 10) has been chosen to define the most appropriate kernel for parameters evaluation, since not-null skewness values are representative of non-symmetric/non-normal distributions. Skewness can be defined as:

$$\mathrm{Sk} = \frac{E(x-\mu)^3}{\sigma^3} \tag{10}$$

where μ and σ are, respectively the mean and the standard deviation of the distribution and $E(t)$ represents the expected value of the quantity t.

The proposed approach is that a window size that causes a deviation of skewness' value from the pattern should been chosen as the most suitable window size for parameters elaboration. We suggest, to underline the work assumptions, that this deviation should refer to a stationary point (extreme skewness value) representing an higher asymmetry on the topographic attribute distribution, therefore a better suitability of the dataset to be used for thresholding based on analysis of defined divergence from normality.

For our elaborations, we should note that openness evaluated at small scale (n=3) for both areas tends to produce normally shaped distributions (skewness near zero). The increasing of the window scale causes a progressive skewing of the distribution toward the left (increasing negative values for the skewness) until a minimum value is reached (approximately n=15), then the distribution moves slightly back toward normality (Fig. 4a,b). Difference on skewness dynamics on the two areas for curvature depends on the higher morphology complexity on the Cordon basin (El. A. Fig. 2),

HESSD
7, 9327–9365, 2010

where small windows sizes cause a too high detection of noises not necessarily related to channelized processes. For the Cordon area, we can observe that the increasing of the window scale determines a progressive normalization of values (skewness increases toward 0). For n=7, a change of slope of this increasing is registered (Fig. 4a). On the Miozza basin, instead, curvature skewness follows openness' but the minimum value is reached faster (n=11 for curvature respect n=15 for openness) (Fig. 4b).

In the course of finding extreme points, a useful tool is the differential calculus that provides a description of the rate of change of a function. According to its main definition, an inflection point refers to a point at which the derivative of the representative function vanishes. For each of our skewness dataset, we evaluate a parametric fitting by using high order polynomials to obtain a function $\text{sk}^*=f(n)$ representing the continuous variation of skewness according to the kernel size (n). The polynomial order has been iteratively chosen in order to provide a curve having at least a derivative at one point n in the domain of f included within the adopted kernel size range (3–33).

We suggest that the optimum kernel size should refers to the minimum n value determining the vanishing of the skewness first derivative (Fig. 5a,b). For minimum curvature, this value refers to n=11.56 for the Cordon area (El. i in Fig. 5a) and n=10.54 for the Miozza one (El. ii in Fig. 5b). Derivative vanishing for positive and negative openness for the Cordon area, is registered at n=12.20 and n=17.55, respectively. On the Miozza basin, positive and negative openness derivatives vanish, respectively for n=12.27 and 16.79 (El. ii in Fig. 5b).

For topographic parameters elaboration, the kernel size has to be an integer odd number, therefore stationary point values have been rounded to the closest odd integer. According to the proposed procedure, a kernel of n=11 has been chosen for minimum curvature on both areas. To give homogeneity to the evaluation of the parameter among and nadir angles, the mean value between the positive and negative openness' stationary points coordinates (14.87 and 14.53 for the Cordon and the Miozza site, respectively) has been rounded to n=15 for openness maps evaluation.

Discussion Paper | Discussion Paper | Discussion Paper | Discussion Paper |

HESSD

7, 9327–9365, 2010

Channel network identification from high-resolution DTM: a statistical approach

G. Sofia et al.

One should note that for both the study areas, according to this methodology, the same windows sizes have been chosen, without any subjective decision.

5 Upslope area weighting procedure

For the present work the Quinn' (1991) flow accumulation algorithm was modified using a weight factor W dependent on local morphology:

$$A_w = f(W, r) \tag{11}$$

where A_w is the weighted upslope contribution area for a given pixel and $r(x, y)$ is the pixel location on the DTM. The main difference from a conventional MDF flow accumulation is to provide a map of W, directly related to geomorphologic form, where surface concavities and convexities are detected.

The weighted upslope area is an implicit description of how much water the upslope area can accumulate according to its degree of convergence. Given a defined upslope value, the weighted upslope amount is depending both on upslope contributing area and local convergence of morphology, represented by a weight matrix W (Eq. 16, Figs. 7d and 8d) identified through normalized values of openness and curvature. If a pixel relies on a convergent morphology, the value of upslope area for that pixel will be increased proportionally to its degree of convergence, while if it lies on divergent morphology, its upslope value will be diminished.

For maps normalization, we evaluated for each attribute map a Quantile-Quantile plot (QQ-plot) (Fig. 6a). This graphical operator compares ordered values of a variable with quantiles of a specific theoretical distribution (here Gaussian) representing the relative likelihood of this random variable to occur at a given point in the observation space. The deviation from a straight line indicates a deviation of the probability density function from the Gaussian and therefore deviation of the values from the overall pattern of points. In the work of Lashermes et al. (2007) and Passalacqua et al. (2010a,b) QQ-plots of landform curvature were used to objectively define curvature thresholds

HESSD
7, 9327–9365, 2010

Channel network identification from high-resolution DTM: a statistical approach

G. Sofia et al.

for channel network extraction. They suggested that the deviation from the normal distribution records an approximate break in which higher values delineate well organized valley axes and lower values record the disordered occurrence of localized convergent topography. Although maps of openness resemble images of shaded relief and slope angle, they actually represent surface concavities and convexities. Therefore in this study we suggested that the deviation from the normal distribution recorded both for openness (ψ_L and ϕ_L) and C_{min} QQ-plots represents the likely threshold for channels identification. For ψ_L, we consider the break on higher values (right tail of distribution), while for ϕ_L, we considered the break for lower values – left tail – (Eqs. 12 and 13). For C_{min} we evaluated the break on negative side (El. i in Fig. 6a) that, following Evans' approach, corresponds to convergent topography (Evans, 1979; Wood, 1996) (Eq. 14). According to these formulation channel are identified where

$$\psi_L > \text{QQ-plot}_{\text{thr}} \tag{12}$$

$$\phi_L < \text{QQ-plot}_{\text{thr}} \tag{13}$$

$$C_{\text{min}} < \text{QQ-plot}_{\text{thr}} \tag{14}$$

where the term "thr" (threshold) is related to the value corresponding to the break in the QQ-plot (El. i in Fig. 6a) evaluated for each map.

Maps normalization has been evaluated according to $\text{QQ-plot}_{\text{thr}}$ using the procedure

$$N_{\text{TA}} = f\left(\frac{1}{\text{QQ plot}_{\text{thr}}}, \text{TA}_{(x,y)}\right) \tag{15}$$

where N_{TA} stands for the normalized topographic attribute considered (openness or curvature) for a given pixel and $\text{TA}_{(x,y)}$ is the topographic attribute at the pixel of interest (Fig. 6c).

HESSD
7, 9327–9365, 2010

The obtained weight grid for upslope area weighting procedures (Figs. 7d and 8d) refers to:

$$W = \frac{\left(N_{C_{\min}}\right) \cdot \left(N_{\psi_L}\right)}{\left(N_{\phi_L}\right)} \tag{16}$$

where N stands for normalization procedure for each topographic attribute map according to Eq. (15). The normalized positive openness map appears to be on the form $1/N\phi_L$ in order to assign higher values to convergent topography as for other maps.

6 Network detection

Field surveyed channel heads for the study area show that observed contributing areas vary significantly and this suggests that a constant value for network extraction might not be a good assumption (Passalacqua et al., 2010b). Average contributing area can be used to define thresholds, but the resulting drainage densities are too high (Passalacqua et al., 2010b). Accurate objective location of channel network from DTMs remains therefore a challenge. For the present work we proposed a sound method to identify these features using an objective threshold based on statistical values of distributions and shape descriptors. The effectiveness of similar approach for feature extraction have been proved by Pirotti and Tarolli (2010) and Passalacqua et al. (2010a,b). We suggest that channel network can be identified by thresholds dependent on the weighted upslope area values distribution. In order to identify this threshold, the weighted upslope area has been standardized according to a z-score procedure, indicating how many standard deviations each observation is above or below the mean.

The standard score (z-score) is a dimensionless quantity and for the i-th observation of a random variable x at a point i is given by:

Discussion Paper | Discussion Paper | Discussion Paper | Discussion Paper |

HESSD

7, 9327–9365, 2010

Channel network identification from high-resolution DTM: a statistical approach

G. Sofia et al.

$$z_i = \frac{x_i - \mu}{\sigma} \tag{17}$$

where μ and σ are, respectively the mean and the standard deviation of the distribution.

Values that are larger than the mean have positive z-scores and values that are smaller than the mean have negative z-scores. If a value equals the mean, then x_i has a z-score of 0.

This normalization allows comparison of observations from different distributions. Z-score transformation changes the central location of the distribution and the average variability of the distribution, but it does not change its skewness or kurtosis.

In order to obtain a threshold that could maintain the characteristic of clear descriptor of distribution shape and its independency from sample size, we chose to define the threshold for channel head and network identification at z-score equal to 0. Channel network is therefore identified by those pixels that satisfy the relation

$$ZA_\mathrm{w} > 0 \tag{18}$$

where ZA_w is the z-score of the weighted upslope area (Eq. 17) at each pixel.

7 Noise filtering

Direct application of openness and curvature independently produce typically segmentation of the resulting raster, because of the numerous local convergences that exist in real surfaces due to inherent noise. The use of weighted upslope area, allows a better connection, but noises are still relevant. While on areas with a low degree of morphological complexity (Miozza), noises can be easily discarded on the produced map through simple filtering based on the majority of contiguous neighboring cells, when the procedure is applied to areas with complex morphology (Cordon, Fig. 2), noise detection becomes more challenging. One opportunity to discard false positives (noises) is to analyze those regions that show high fragmentation and to analyze the magnitude of this fragmentation in order to mark areas with high degree of morphological

Discussion Paper | Discussion Paper | Discussion Paper | Discussion Paper |

HESSD

7, 9327–9365, 2010

Channel network identification from high-resolution DTM: a statistical approach

G. Sofia et al.

disorganization. It is generally difficult to obtain relevant markers automatically without any interaction by the user, therefore we suggest an approach that can be useful, once the proposed automatic procedure has been applied, to interactively discard localized patterns and misleading noisy cells which do not actually represent the features. This approach is not fully automatic, but it can be used to assist interactively the interpreter/user on the task of identifying the network.

We suggest that that noises can be related to higher randomness of values of the original elevation data, while concavities related to channels refer to patterns with a better organization. We suggest that a good representation of the elevation organization can be identified through the analysis of water movement for each cell. Flow is defined by any cell within a neighborhood that has a higher value than the processing cell. The output map that results from the function represent the pattern of the flow into each cell. In order to test the degree of organization of this map, we evaluate a statistical measure of randomness, referenced as Entropy (Gonzales et al., 2003). We produce a raster map where each output pixel contains the entropy value of the nearest neighborhood according to the formulation

$$\text{Entropy} = -\sum p_i \cdot \log p_i \tag{19}$$

where p_i is the proportion of pixels that are assigned to each class.

For class evaluation, flow convergence values have been converted to unsigned 8-bit integer so that the pixel values become discrete and directly correspondent to a bin value on the range 1–255 (Gonzales et al., 2003).

To maintain homogeneity with the full procedure, cells neighborhood has been defined according to an average window size (n=13) between the chosen ones for curvature and openness.

We suggest to observe the entropy degree on areas where extraction produce not clear results and to discard those extractions obtained in areas with values of entropy higher than the average (Fig. 9b). According to this analysis, some noises (El. i, ii in Fig. 9) can be discarded. Element iii in Fig. 9 refers to a channel referenced on maps

HESSD
7, 9327–9365, 2010

but actually not active on the area, therefore it has not been considered for quality evaluation.

Once we applied the two filtering procedures (majority filter for the Miozza basin and entropy analysis for the Cordon area) the remaining network needs a connection procedure. Considering a pour point (maximum value of flow convergences) we identified the most suitable (shortest) flow path from each channel head to the pour point. This path has been identified as the least accumulative cost distance to the pour point over a cost surface set as the Euclidean distance of each pixel from the correct extraction. For a fuller discussion of accumulated costs surfaces methods and representational accuracy see Douglas (1994) and Eastman (1989). Similar approach to network connection has been successfully tested in the work of Passalacqua et al. (2010a,b) where channel networks were detected by the use of non linear diffusion and geodesic path.

8 Results and discussion

The final product is a map representing the channel network. The overall quality of the extraction results has been evaluated considering Cohen's k index of agreement (Cohen, 1960) respect to a DGPS surveyed network (Pirotti and Tarolli, 2010).

For accuracy assessment the extracted networks (Figs. 10b and 11b) have been compared with reference channel network surveyed on the study areas (Figs. 10a and 11a).

The quality measure used for this accuracy assessment was defined as

$$k = \frac{P_\mathrm{a} - P_e}{1 - P_e} \tag{20}$$

where P_a is the total agreement probability evaluated according to Eq. (21), and P_e is the agreement probability which is due to chance, according to the formulation in Eq. (22) (Cohen, 1960).

HESSD
7, 9327–9365, 2010

Title Page
Abstract | Introduction
Conclusions | References
Tables | Figures
◀ | ▶
Back | Close
Full Screen / Esc
Printer-friendly Version
Interactive Discussion

$$P_a = \sum_{i=1}^{I} P(x_{ii}) \tag{21}$$

$$P_e = \sum_{i=1}^{I} P(x_{.i})P(x_{i.}) \tag{22}$$

where i is the number of class values, $P(x_{.i})$, $P(x_{i.})$ are the columns and rows marginal probabilities, respectively and $P(x_{ii})$ are the agreeing extracted values.

Perfect agreement results in a Cohen's k value of 1.0, while a value of 0 indicates a level of agreement due to chance alone. Although no definitive reference scale exists for Cohen's k values for hydrological applications, prior reports of the index in other fields suggested a scale for Cohen's k values and their level of agreement between datasets: values of k lower than 0.2 indicate slight agreement, 0.20–0.40 represent a fair agreement, 0.40–0.60 moderate agreement, 0.60–0.80 substantial agreement, and 0.80–1.00 indicates almost perfect agreement (Landis and Koch, 1977).

For indexes evaluation, buffer zones were generated around the extracted network as well as the reference one. The chosen buffer width was set to 5 m according to a previous work carried out on the Cordon area using the same dataset, where analysis of results had been performed using the same quality measure (Pirotti and Tarolli, 2010). To maintain homogeneity, the same buffer width has been considered for both the Cordon and the Miozza case study.

The extraction procedure generates a network characterized by a substantial agreement between extracted features and reference ones for both applications: Cohen's k is 0.78 and 0.63 for the Cordon area and the Miozza basin, respectively (Table 1).

HESSD

7, 9327–9365, 2010

9 Final remarks

This work analyzed a statistical approach to a combination of topographic attributes for channel network identification in a complex mountainous terrain. Our primary focus has been to develop and present a method that was capable to accurately describe the drainage network using objective thresholds without an a-priori knowledge of the study area. The methodology includes two main aspect: (a) normalization of openness and minimum curvature maps according to their QQ-plot$_{thr}$ and their combination in order to produce a weight matrix that highlights potential surface convergences and (b) a thresholding procedure based on statistical analysis of values distribution applied to weighted upslope area. The methodology has been applied first to a rectangular area on a study site and then to a fully-organized basin used as test site. Both extracted features were then compared with the field surveyed networks.

Field observed contributing areas to channel heads vary significantly and a constant contributing area applied to channel network extraction is not suitable for basins where channel network initiation depends on different morphological processes. The use of statistic operators as objective indexes for maps normalization and thresholding procedures results on a network correctly delineated without the need to subjectively chose an area threshold parameter derived from field survey. Applying the proposed procedure using normalized landform attributes for surface convergence identification allows furthermore the definition of a drainage network strongly consistent with surface morphology. Automatic detection of plausible network based on thresholding operations was demonstrated as efficient in terms of time consumption and valid to associate shapes and pattern derived from high resolution topography with real topographic signature of flow processes. The approach, anyway, present some limits, especially in areas with complex morphology where also other surface features not related to channel networks are detected. Network extraction carried out using openness and curvature independently, could be capable of representing an overall channel network pattern, however such methods show some flaws detecting some localized patterns and

HESSD

7, 9327–9365, 2010

Channel network identification from high-resolution DTM: a statistical approach

G. Sofia et al.

misleading noisy cells which do not actually represent the features, and they includes some gaps causing difficulties on connecting the extracted feature into a meaningful network without an a-priori knowledge of the environment. These parameters yet are able to provide a quantitative and qualitative description of the network and to provide overall information about position and orientation of local convergences. The analysis of surface entropy has been proven in this case to be a useful tool to assist the user on discarding doubtful extractions, such those reached at the top of our study area and it can be used to interactively assist the interpreter/user on the task of automatic network mapping. Finally, shortest cost path procedures applied to the filtered maps, allow the definition of a meaningfully connected network. The result are accurate and promising for practical applications.

Acknowledgements. This work was partially supported by the Interreg IIIB Spazio alpino Project CATCHRISK (Mitigation of hydrogeological risk in Alpine catchments) and by the Italian Ministry of University and Research – GRANT PRIN 2005 "National network of experimental basins for monitoring and modelling of hydrogeological hazard". The authors thank the Regional Service of Agricultural, Natural, Forestry and Mountain Resources of the Friuli Venezia Giulia Region for collaboration during the field surveys. The airborne LiDAR data were elaborated by University of Udine within the Interreg IIIA Italy–Slovenia project. Computer resources were provided by the Interdepartmental Research Center for Cartography, Photogrammetry, Remote Sensing and GIS, at the University of Padova.

References

Ackermann, F.: Airborne laser scanning – present status and future expectations, IS-PRN J. Photogram. Remote Sens., 54, 64–67, 1999.

Albani, M., Klinkenberg, B., Andison, D. W., and Kimmins, J. P.: The choice of window size in approximating topographic surfaces from digital elevation models, Int. J. Geogr. Inf. Sci., 18(6), 577–593, 2004.

Band, L. E.: Topographic partition of watersheds with digital elevation models, Water Resour. Res., 22(1), 15–24, 1986.

HESSD

7, 9327–9365, 2010

Bartels, M., Wei, H., and Mason, D. C.: Wavelet packets and cooccurrence matrices for texture-based image segmentation, IEEE International Conference on Advanced Video and Signal-Based Surveillance, 1, 428–433, 2005.

Beven K. J. and Kirkby, M. J.: A physically based, variable contributing area model of basin hydrology, Hydrol. Sci. Bull., 24, 43–69, 1979.

Briese, C.: Breakline Modelling from Airborne Laser Scanner Data, PhD Thesis, Institute of Photogrammetry and Remote Sensing, Vienna University of Technology, Vienna, 2004.

Broscoe, A. J.: Quantitative analysis of longitudinal stream profiles of small watersheds. Office of Naval Research, Project NR 289–042, Technical Report No. 18, Department of Geologyy, Columbia University, New York, 1959.

Cavalli, M. and Marchi, L.: Characterisation of the surface morphology of an alpine alluvial fan using airborne LiDAR, Nat. Hazards Earth Syst. Sci., 8, 323–333, doi:10.5194/nhess-8-323-2008, 2008.

Cohen, J.: A coefficient of agreement for nominal scales, Educ. Psychol. Meas., 20, 37–46, 1960.

Dalla Fontana, G. and Marchi, L.: Slope-area relationships and sediment dynamics in two alpine streams, Hydrol. Process., 17(1), 73–87, 2003.

Desmet, P. J. J. and Govers, G.: Comparison of routing algorithms for digital elevation models and their implications for predicting ephemeral gullies, Int. J. Geogr. Inf. Syst., 10, 311–331, 1996.

Dietrich, W. E. and Dunne, T.: The channel head, in: Channel Network Hydrology, edited by: Beven, K. and Kirkby, M. J., Wiley, Chichester, 175–219, 1993.

Douglas, D. H.: Least cost path in GIS using an accumulated cost surface and slope lines, Cartographica, 31, 37–51, 1994.

Duda, R. O., Hart, P. E., and Stork, D. G.: Pattern Classification, Wiley, New York, 2001.

Eastman, J. R.: Pushbroom algorithms for calculating distances in raster grids [online], Proceedings of the International Symposium on Computer-Assisted Cartography, Autocarto, 9, 288–297, 1989.

Ehlschlaeger, C.: Using the A* Search Algorithm to Develop Hydrologic Models from Digital Elevation Data, Proceedings of International Geographic Information Systems (IGIS) Symposium, Baltimore, MD, USA, 275–281, 1989.

Endreny, T. A. and Wood, E. F.: Maximizing spatial congruence of observed and DEM-delineated overland flow networks, Int. J. Geogr. Inf. Syst., 17, 699–713, 2003.

Eshani, A. H. and Quiel, F.: Geomorphometric feature analysis using morphometric parameterization and artificial neural networks, Geomorphology, 99, 1–12, 2008.
Evans, I. S.: General geomorphology, derivatives of altitude and descriptive statistics, in: Spatial Analysis in Geomorphology, edited by: Chorley, R. J., Methuen & Co. Ltd, London, 17–90, 1972.
Evans, I. S.: An integrated system of terrain analysis and slope mapping, Final report on grant DA-ERO-591–73-G0040, University of Durham, Durham, England, 1979.
Evans, I. S.: An integrated system of terrain analysis and slope mapping, Z. Geomorphol., Suppl-Bd. 36, 274–295, 1980.
Florinsky, I. V.: Accuracy of local topographic variables derived from digital elevation models, Int. J. Geogr. Inf. Sci., 12(1), 47–61, 1998.
Gallant, J. C. and Wilson, J. P.: Primary topographic attributes, in: Terrain Analysis: Principles and Applications, edited by: Wilson, J. P. and Gallant, J., John Wiley & Sons Inc., New York, 51–85, 2000.
Gonzalez, R. C., Woods, R. E., and Eddins, S. L.: Digital Image Processing Using MATLAB, chap. 11, Prentice Hall, New Jersey, 11, 2003.
Güntner, A., Seibert, J., and Uhlenbrook, S.: Modeling spatial patterns of saturated areas: An evaluation of different terrain indices, Water Resour. Res., 40, W05114, doi:10.1029/2003WR002864, 2004.
Hart, P. E., Nilsson, N. J., and Raphael, B.: A formal basis for the heuristic determination of minimum cost paths, IEEE T. Syst. Sci. Cyb., 4, 100–107, 1968.
Horn, B. K. P.: Hill shading and the reflectance map, Proceedings IEEE, 69(1), 14–47, 1981.
Kraus, K. and Pfeifer, N.: Advanced DTM generation from LIDAR data, Int. Archives Photogrammetry Remote Sens., XXXIV-3/W4, 23–35, 2001
Landis, J. R. and Koch, G. G.: The measurement of observer agreement for categorical data, Biometrics, 33, 159–174, 1977.
Lashermes, B., Foufoula-Georgiou, E., and Dietrich, W. E.: Channel network extraction from high resolution topography using wavelets, Geophys. Res. Lett., 34, L23S04, doi:10.1029/2007GL031140, 2007.
McGlynn, B. L. and McDonnell, J. J.: Quantifying the relative contributions of riparian and hillslope zones to catchment runoff, Water Resour. Res., 39(11), 1310, 2003.
McMaster, K. J.: Effects of digital elevation model resolution on derived stream network positions, Water Resour. Res., 38(4), 1042, 2002.

Metz, M., Mitasova, H., and Harmon, R. S.: Accurate stream extraction from large, radar-based elevation models, Hydrol. Earth Syst. Sci. Discuss., 7, 3213–3235, doi:10.5194/hessd-7-3213-2010, 2010.

Mitasova, H. and Hofierka, J.: Interpolation by regularized spline with tension: II. application to terrain modeling and surface geometry analysis, Math. Geol., 25, 641–655, 1993.

Molloy, I. and Stepinski, T. F.: Automatic mapping of valley networks on Mars, Comput. Geosci., 33, 728–738, 2007.

Montgomery D. R. and Dietrich, W. E.: Where do channels begin?, Nature, 336, 232–234, 1988.

Montgomery, D. R. and Dietrich, W. E.: A physically based model for the topographic control on shallow landsliding, Water Resour. Res., 30(4), 1153–1171, 1994.

O'Callaghan, J. F. and Mark, D. M.: The extraction of drainage networks from digital elevation data, Comp. Imag. Vis., 28(3), 323–344, 1984.

Orlandini, S., Moretti, G., Franchini, M., Aldighieri, B., and Testa, B.: Path-based methods for the determination of nondispersive drainage directions in grid-based digital elevation models, Water Resour. Res., 39(6), 1144, doi:10.1029/2002WR001639, 2003.

Passalacqua, P., Do Trung, T., Foufoula-Georgiou, E., Sapiro, G., and Dietrich, W. E.: A geometric framework for channel network extraction from lidar: Nonlinear diffusion and geodesic paths, J. Geophys. Res., 115, F01002, doi:10.1029/2009JF001254, 2010a.

Passalacqua, P., Tarolli, P., Foufoula-Georgiou, E.: Testing space-scale methodologies for automatic geomorphic feature extraction from LiDAR in a complex mountainous landscape, Water Resour. Res., ISSN 0043-1397, 46, W11535, doi:10.1029/2009WR008812, 2010b.

Pike, R. J. Acevedo, W., and Thelin, G. P.: Some topographic ingredients of a geographic information system, Proceedings, First International Symposium on GIS, 15–18 November, Arlington, Virginia, NASA, Washington, DC, 2, 151–164, 1988.

Pirotti, F. and Tarolli, P.: Suitability of LiDAR point density and derived landform curvature maps for channel network extraction, Hydrol. Process., 1187–1197, doi:10.1002/hyp.7582, 2010.

Prima, O. D. A., Echigo, A., Yokoyama, R., and Yoshida, T.: Supervised landform classification of Northeast Honshu from DEM-derived thematic maps, Geomorphology, 78, 373–386, 2006.

Prosser, I. P. and Abernethy, B.: predtcing the topographic limits of gully network using a digital terrain model and process thresholds, Water Resour. Res., 32, 2289–2298, 1996.

HESSD
7, 9327–9365, 2010

Quinn, P., Beven, K., Chevallier, P., and Planchon, O.: The prediction of hillslope flow paths for distributed hydrological modeling using digital terrain models, Hydrol. Process., 5, 59–79, 1991.
Schoorl, J. M., Sonneveld, M. P. W., and Veldkamp A.: Threedimensional landscape process modelling: the effect of DEM resolution, Earth Surf. Proc. Land., 25, 1025–1034, 2000.
Schwanghart, W. and Kuhn, N. J.: TopoToolbox: a set of Matlab functions for topographic analysis, Environ. Modell. Softw., 25, 770–781, 2010.
Seibert, J. and McGlynn, B. L.: A new triangular multiple flow-direction algorithm for computing upslope areas from gridded digital elevation models, Water Resour. Res., 43, W04501, doi:10.1029/2006WR005128, 2007
Shary, P. A., Sharaya, L. S., and Mitusov, A. V.: Fundamental quantitative methods of land surface analysis, Geoderma, 107, 1–32, 2002.
Slatton, K. C., Carter, W. E., Shrestha, R. L., and Dietrich, W. E.: Airborne laser swath mapping: achieving the resolution and accuracy required for geosurficial research, Geophys. Res. Lett., 34, L23S10, doi:10.1029/2007GL031939, 2007.
Tarboton, D. G.: A new method for the determination of flow directions and upslope areas in grid digital elevation models, Water Resour. Res., 33, 309–319, 1997.
Tarboton, D. G.: Terrain Analysis Using Digital Elevation Models in Hydrology, ESRI Users Conference, San Diego, 7–11 July, 2003.
Tarboton, D. G. and Ames, D. P.: Advances in the Mapping of Flow Networks from Digital Elevation Data. World Water and Environmental Resources Congress, ASCE, Orlando, Florida, 2001.
Tarboton, D. G., Bras, R. L., and Rodriguez-Iturbe, I.: on the extraction of channel network from digital elevation data, Hydrol. Process., 5, 81–100, 1991.
Tarolli, P. and Dalla Fontana, G.: High resolution LiDAR-derived DTMs: some applications for the analysis of the headwater basins' morphology, International Archives of Photogrammetry, Remote Sensing and Spatial Information Sciences, 36(5/C55), 297–306, 2008.
Tarolli, P. and Dalla Fontana, G.: Hillslope to valley transition morphology: new opportunities from high resolution DTMs, Geomorphology, 113, 47–56, 2009.
Tarolli, P. and Tarboton, D. G.: A new method for determination of most likely landslide initiation points and the evaluation of digital terrain model scale in terrain stability mapping, Hydrol. Earth Syst. Sci., 10, 663–677, doi:10.5194/hess-10-663-2006, 2006.

Tarolli, P., Arrowsmith, J. R., and Vivoni, E. R.: Understanding earth surface processes from remotely sensed digital terrain models, Geomorphology, 113, 1–3, 2009.
Thommeret, N., Bailly, J. S., and Puech, C.: Extraction of thalweg networks from DTMs: application to badlands, Hydrol. Earth Syst. Sci., 14, 1527–1536, doi:10.5194/hess-14-1527-2010, 2010.
Wemple, B. C., Jones, J. A., and Grant, G. E.: Channel network extension by logging roads in two basins, wester cascades, Oregon, Water Resour. Bull., 32(6), 1195–1207, 1996.
Wilson, M. F. J., O'Connel, B., Brown, C., Guinan, J. C., and Grehan, A. J.: Multiscale terrain analysis of multibeam bathymetry data for habitat mapping on the continental slope, Mar. Geod., 30, 3–35, 2007.
Wolock, D. M. and McCabe, G. J.: Comparison of single and multiple flow direction algorithms for computing topographic parameters, Water Resour. Res., 31, 1315–1324, 1995.
Wood, J.: The Geomorphological Characterisation of Digital Elevation Models, PhD, University of Leicester, Leicester, 1996.
Wood, J.: Geomorphometry in LandSerf, in: Developments in Soil Science, edited by: Hengl, T. and Reuter, H. I., chap. 14, Elsevier, 33, Geomorphometry – Concepts, Software, Applications, doi:10.1016/S0166-2481(08)00014-7, 333–349, 2009.
Yokoya, N. and Levine, M. D.: Range image segmentation based on differential geometry: a hybrid approach, IEEE Trans. Pattern Anal. Mach. Intell., 2(6), 643–649, 1989.
Yokoyama, R., Sirasawa, M., and Pike, R.: Visualizing topography by openness: a new application of image processing to digital elevation models, Photogramm. Eng. Remote Sens., 68(3), 257–265, 2002.
Yuan, X., Hu, L., Buckles, B. P., Steinberg, L., and Sarma, V.: An Adaptive Method for the Construction of Digital Terrain Model from LiDAR Data, IEEE International Geoscience and Remote Sensing Symposium, Boston, MA, 6–11 July, 2008.
Zevenbergen, L. W. and Thorne, C.: Quantitative analysis of land surface topography, Earth Surf. Proc. Land., 12, 47–56, 1987.

HESSD
7, 9327–9365, 2010

Channel network identification from high-resolution DTM: a statistical approach

G. Sofia et al.

HESSD
7, 9327–9365, 2010

Channel network identification from high-resolution DTM: a statistical approach

G. Sofia et al.

Table 1. Assessment of results: quality index adopted for network extraction (Cohen's k, Eq. 20).

	Cohen's k
Cordon study area	0.78
Miozza basin	0.63

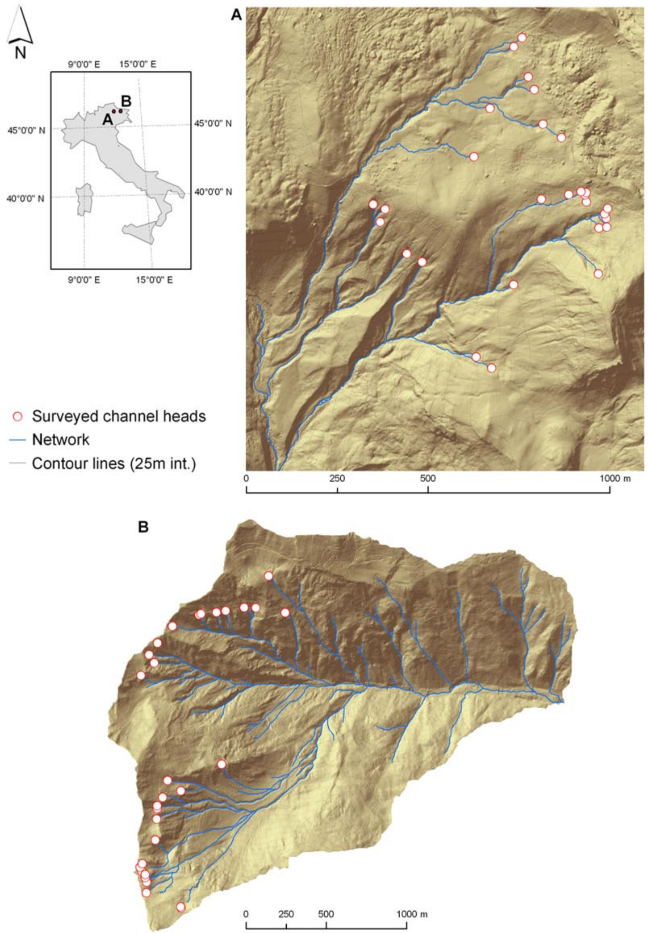

Fig. 1. Maps showing the location of the study area on the Cordon basin **(A)** and the test area on the Miozza basin **(B)**. Drainage network and surveyed channel heads are shown.

HESSD
7, 9327–9365, 2010

Channel network identification from high-resolution DTM: a statistical approach

G. Sofia et al.

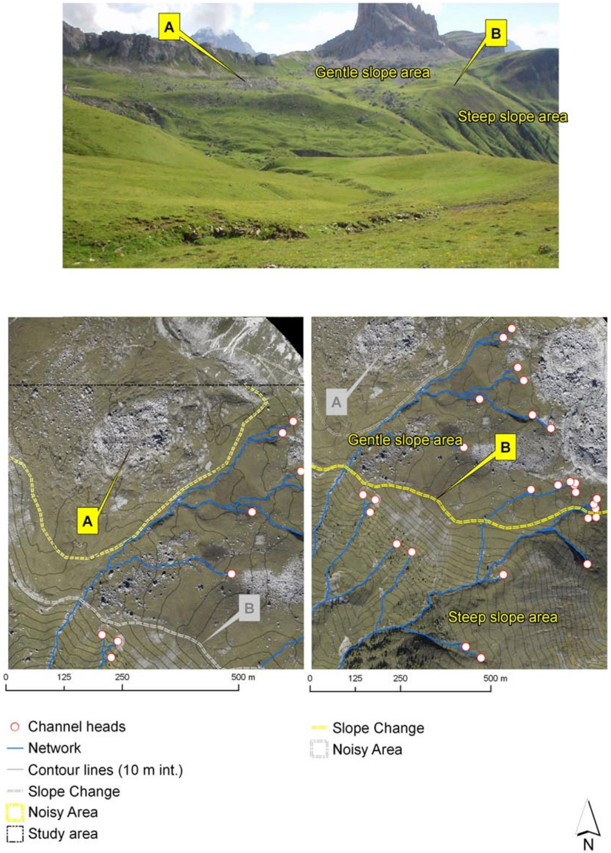

Fig. 2. Example of complex morphology on the upper part of the Cordon basin. The high degree of complexity (A) and the rapid slope change (B) define two of the main issues related to channel network extraction on this area according to topographic parameters and classic thresholding procedure, respectively.

HESSD
7, 9327–9365, 2010

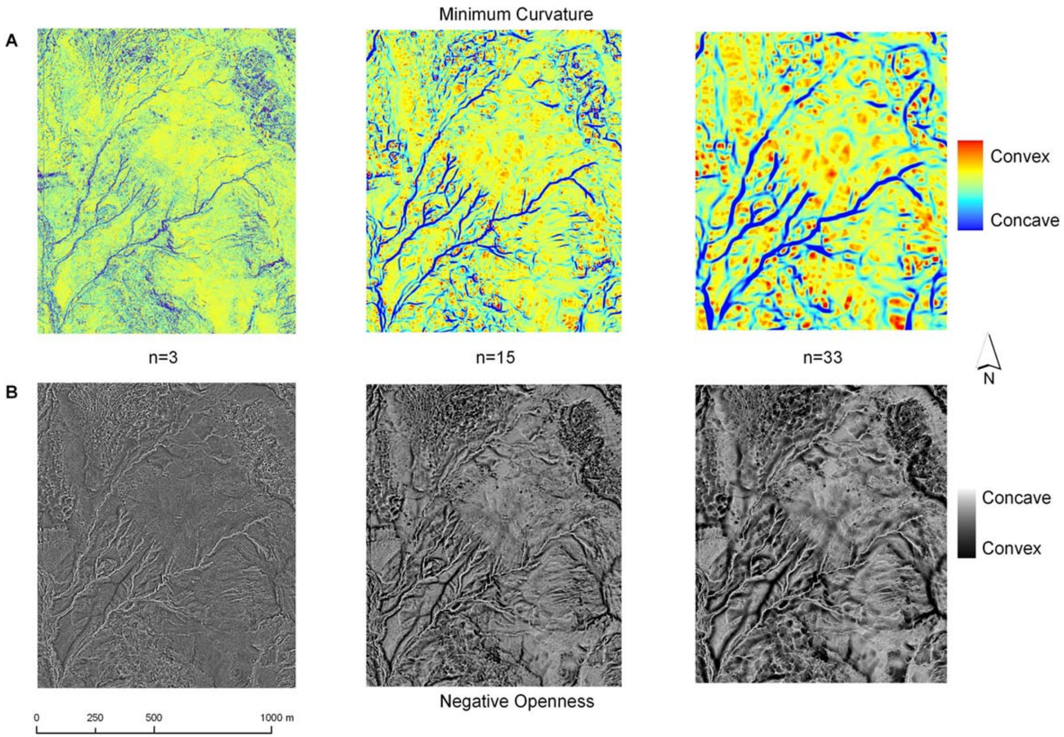

Fig. 3. Example of kernel size effect on minimum curvature **(A)** and negative openness **(B)** for the Cordon study site according to an increasing window size (*n*) of 3, 15 and 33 cells.

HESSD
7, 9327–9365, 2010

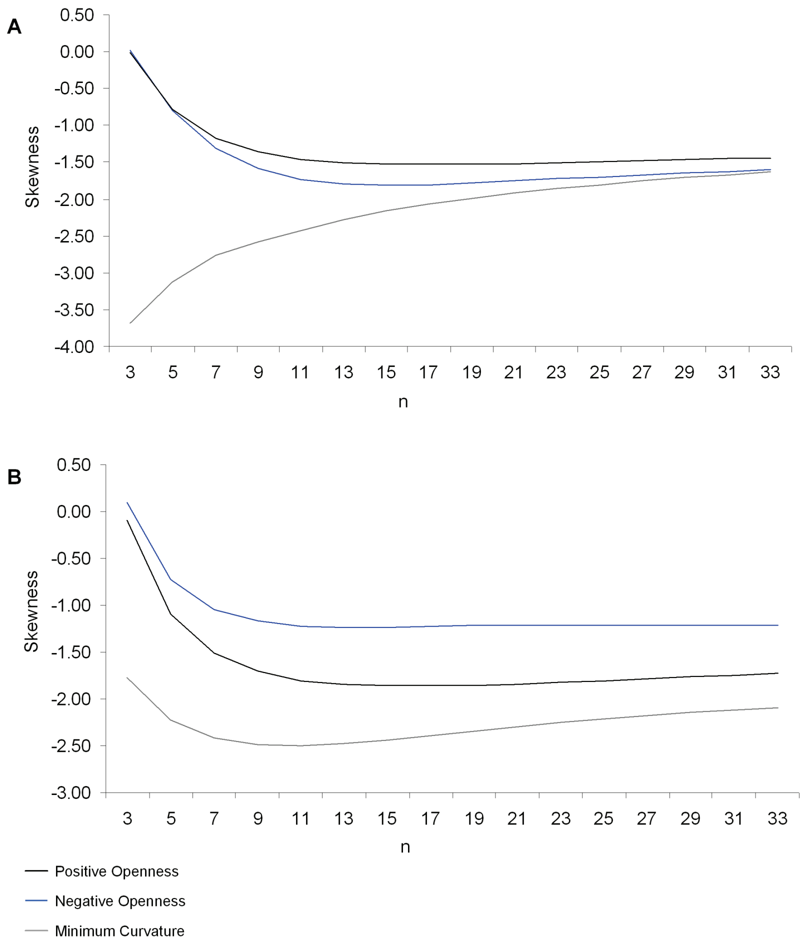

Fig. 4. Skewness for each topographic attribute according to window size (*n*) for the Cordon study site **(A)** and the Miozza basin **(B)**.

HESSD
7, 9327–9365, 2010

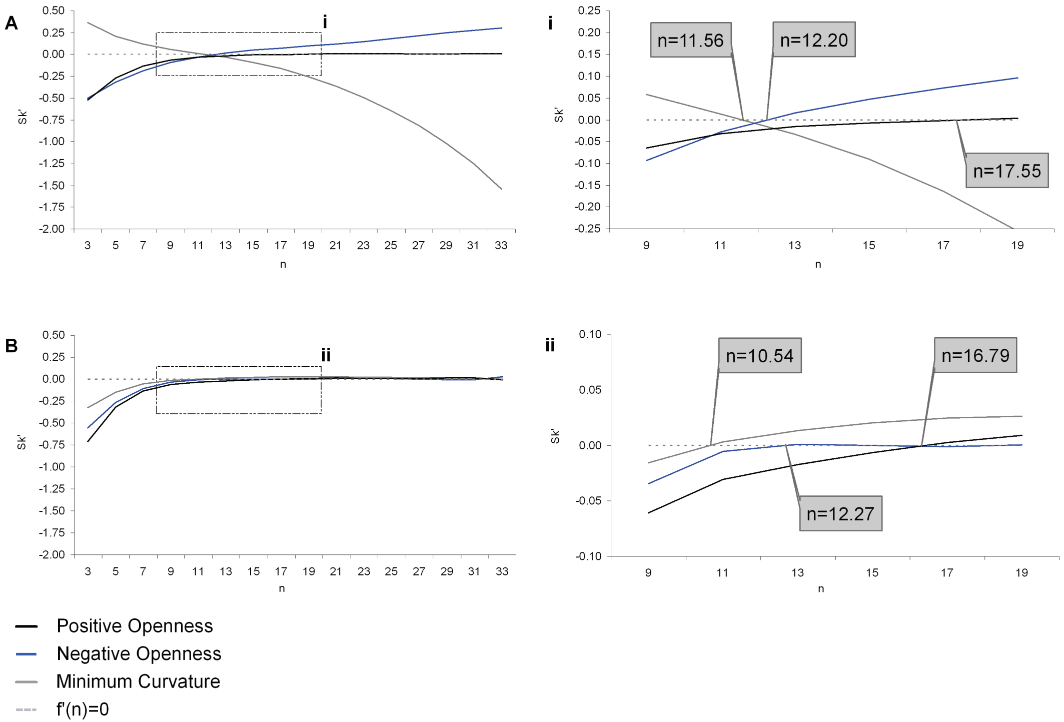

Fig. 5. Derivative for the basic fitting of skewness values for each topographic attribute according to the choice of the window size (n) for curvature and openness evaluation, both for the Cordon study site **(A)** and the Miozza basin **(B)**. Detailed vision of skewness derivative vanishing is showed on the right side of the figure, in *i* for the Cordon evaluation and *ii* for the Miozza one.

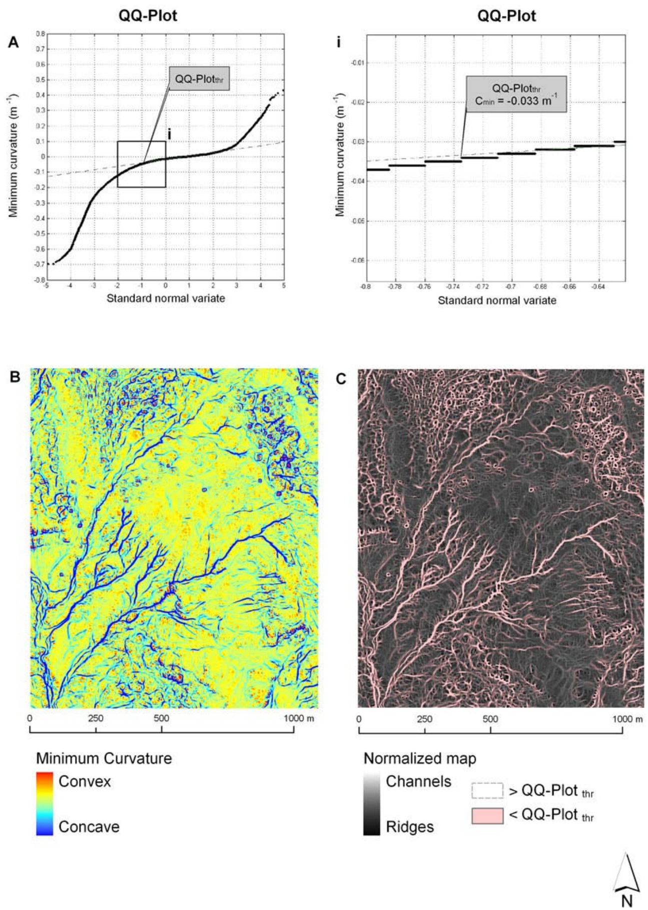

Fig. 6. Cordon study area: topographic attribute map normalization. Example of QQ-plot **(A)** for minimum curvature and identification of threshold **(i)** to apply in order to normalize the map. Minimum curvature for n=9 **(B)** and derived normalized map **(C)** are shown.

HESSD
7, 9327–9365, 2010

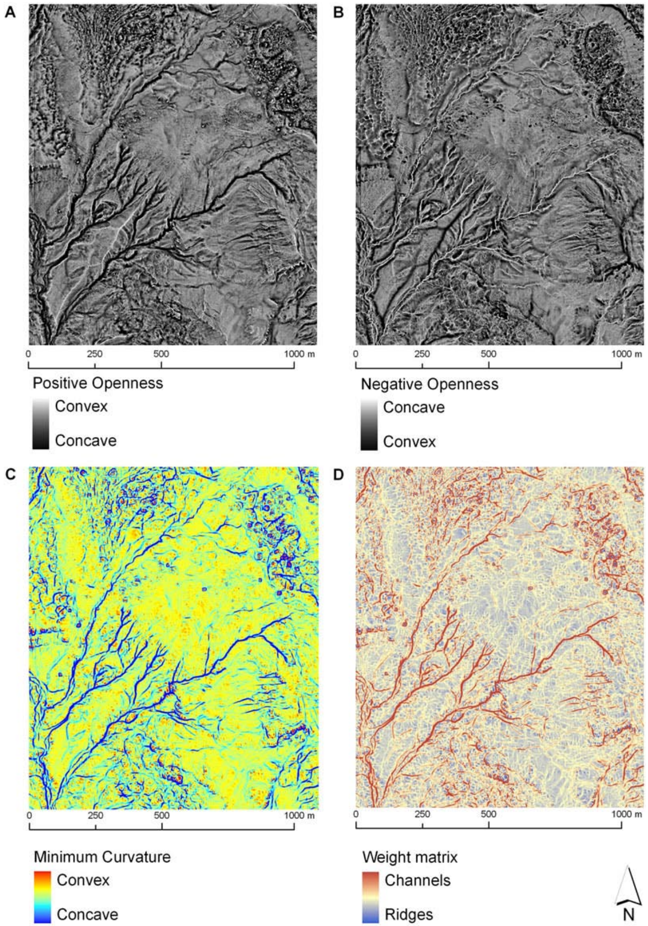

Fig. 7. Cordon study area: positive **(A)** and negative **(B)** openness, minimum curvature **(C)** and weight matrix **(D)** derived through normalization and overlapping.

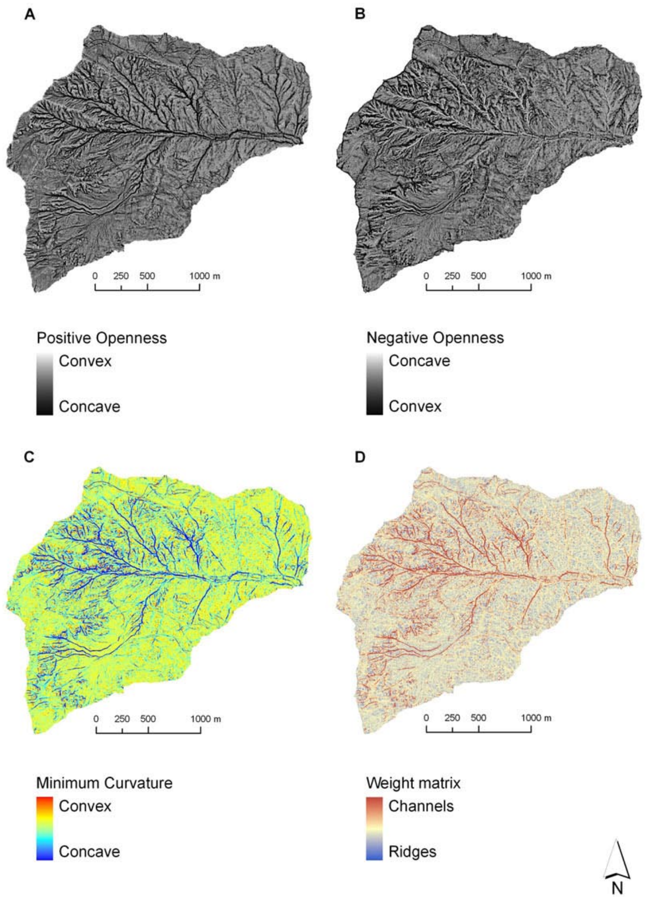

Fig. 8. Miozza basin: positive **(A)** and negative **(B)** openness, minimum curvature **(C)** and weight matrix **(D)** derived through normalization and overlapping.

HESSD
7, 9327–9365, 2010

Channel network identification from high-resolution DTM: a statistical approach

G. Sofia et al.

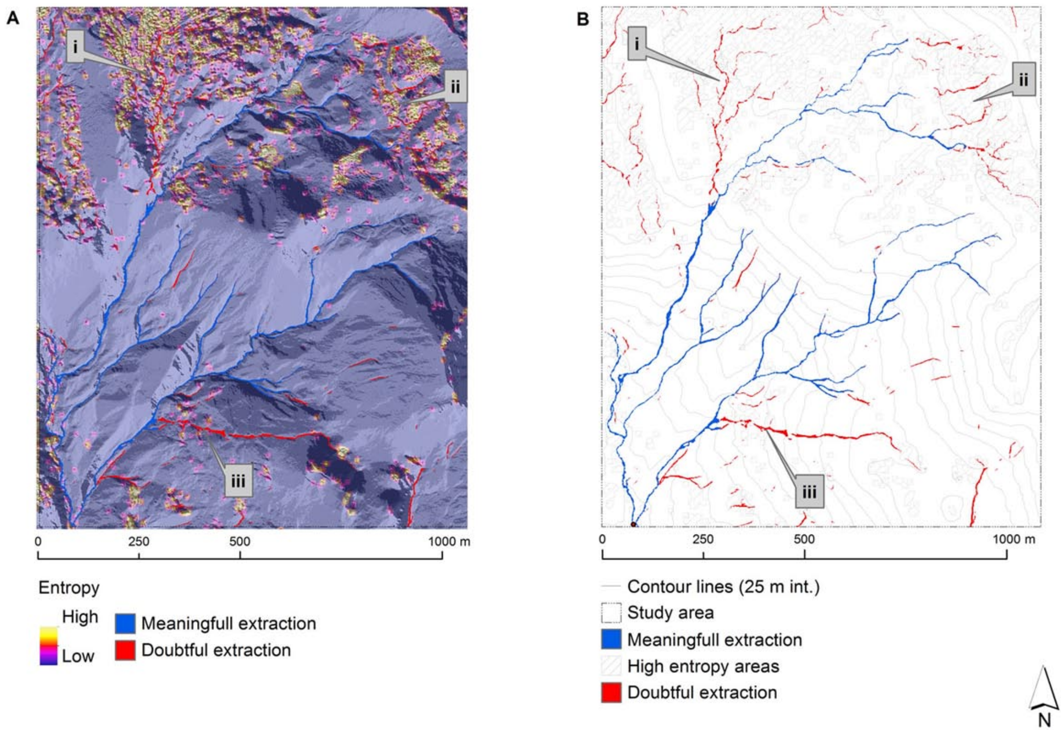

Fig. 9. Cordon study area: local entropy according to flow convergences **(A)** and identification of meaningful (blue) and doubtful (red) pixels **(B)**.

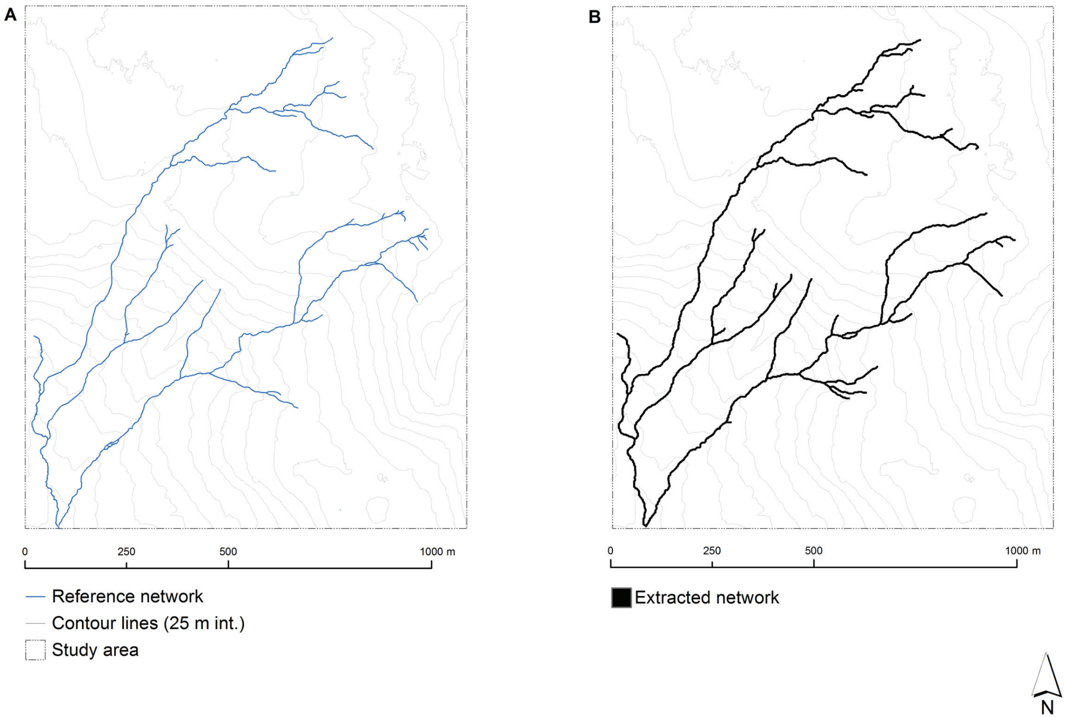

Fig. 10. Cordon study area: reference network **(A)** and network extracted through the proposed methodology **(B)**.

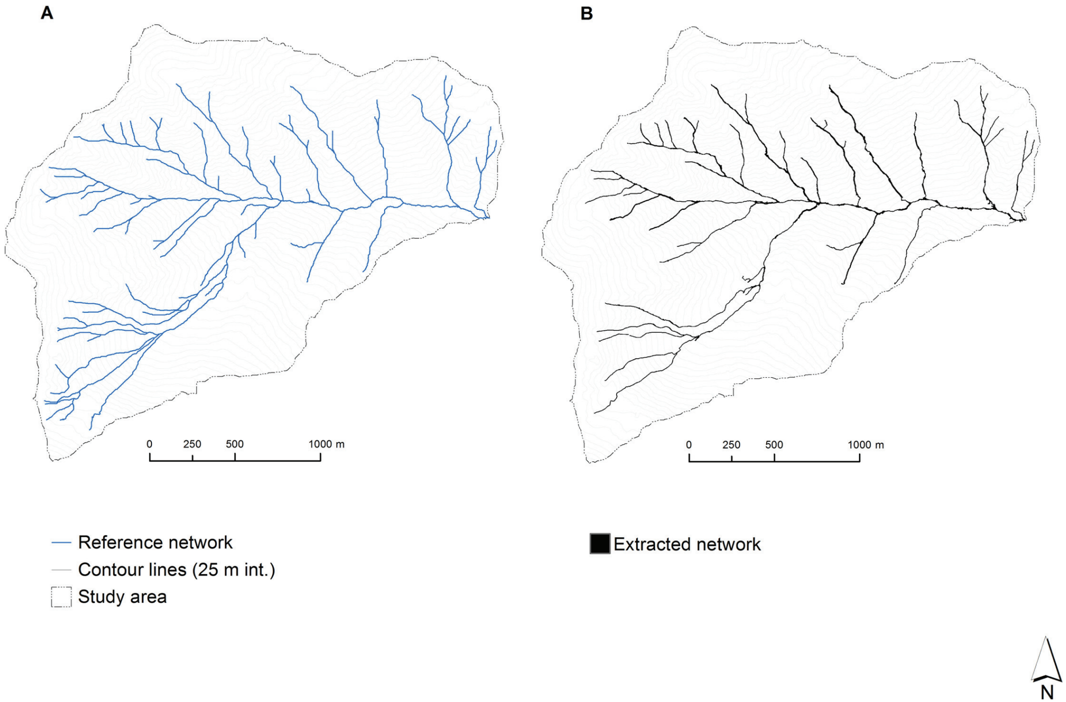

Fig. 11. Miozza basin: reference network **(A)** and network extracted through the proposed methodology **(B)**.

HESSD
7, 9327–9365, 2010

Channel network identification from high-resolution DTM: a statistical approach

G. Sofia et al.